RESEARCH ARTICLE

WILEY

A Bayesian time series model for reconstructing hydroclimate from multiple proxies

Niamh Cahill[1,2] | **Jacky Croke[3]** | **Micheline Campbell[4]** | **Kate Hughes[5]** | **John Vitkovsky[6]** | **Jack Eaton Kilgallen[7]** | **Andrew Parnell[7,8]**

[1]Department of Mathematics and Statistics, Maynooth University, Kildare, Ireland

[2]Irish Climate Analysis and Research UnitS (ICARUS), Maynooth University, Kildare, Ireland

[3]School of Geography, University College Dublin, Dublin, Ireland

[4]School of Biological, Earth and Environmental Sciences, University of New South Wales, New South Wales, Sydney, Australia

[5]Catchment Connections, Queensland, Brisbane, Australia

[6]Department of Environment and Science, Queensland Government, Queensland, Brisbane, Australia

[7]Hamilton Institute, Maynooth University, Kildare, Ireland

[8]Insight Centre for Data Analytics, Maynooth University, Kildare, Ireland

Correspondence
Niamh Cahill, Department of Mathematics and Statistics, Maynooth University, Kildare, Ireland.
Email: Niamh.Cahill@mu.ie

Abstract

We propose a Bayesian model which produces probabilistic reconstructions of hydroclimatic variability in Queensland Australia. The model provides a standardized approach to hydroclimate reconstruction using multiple palaeoclimate proxy records derived from natural archives such as speleothems, ice cores and tree rings. The method combines time-series modeling with inverse prediction to quantify the relationships between a given hydroclimate index and relevant proxies over an instrumental period and subsequently reconstruct the hydroclimate back through time. We present case studies for Brisbane and Fitzroy catchments focusing on two hydroclimate indices, the Rainfall Index (RFI) and the Standardized Precipitation-Evapotranspiration Index (SPEI). The probabilistic nature of the reconstructions allows us to estimate the probability that a hydroclimate index in any reconstruction year was lower (higher) than the minimum (maximum) value observed over the instrumental period. In Brisbane, the RFI is unlikely (probabilities < 5%) to have exhibited extremes beyond the minimum/maximum values observed between 1889 and 2019. However, in Fitzroy there are several years during the reconstruction period where the RFI is likely (>50% probability) to have exhibited behavior beyond the minimum/maximum of what has been observed, during the instrumental period. For SPEI, the probability of observing such extremes prior to the beginning of the instrumental period in 1889 doesn't exceed 30% in any reconstruction year in Brisbane, but exceeds 50% in multiple years in Fitzroy.

KEYWORDS
Bayesian modeling, hydroclimate, multiple proxy, reconstruction

1 | INTRODUCTION

The Australian continent experiences hydroclimatic variability that is regarded as extreme compared to the rest of the world (Dixon et al., 2019; Dowdy et al., 2019). Australia is particularly vulnerable to relatively small changes in rainfall; floods and droughts are common (O'Donnell et al., 2021). Past trends in precipitation showing rainfall increases in many

tropical areas and rainfall decreases in many temperate areas are projected to continue and become more extreme in the future (Head et al., 2014). Increases in the frequency and intensity of extremes will create new pressures and vulnerabilities with the impacts varying geographically and socioeconomically. For example, following repeated Queensland floods, some insurance companies have increased premiums and become less willing to insure houses on floodplains (Suncorp Group, 2013). However, considerable uncertainty remains in relation to how observational extremes (minimum/maximum measurements) fit within the context of past variability, making it difficult to attribute more recent observed variation to natural variability or anthropogenic climate forcing (Cook et al., 2016; Kiem et al., 2020).

To date, hydroclimatic risk in Australia has been assessed using primarily historical instrumental records of rain, evaporation, and streamflow. These instrumental records typically only exist for about the last 100 years at best. Such short records limit the calculation of robust statistics around the baseline risk of extreme events (Armstrong et al., 2020; Tingstad et al., 2014) with potentially catastrophic economic and social consequences. When longer records are included, more low-probability, higher-impact events are identified. For example, under climate boundary conditions similar to present, megadroughts lasting 10–40 years are evident in a 1000-years eastern Australian annual rainfall reconstruction from the Law Dome (LD) ice core record (Vance, 2012). It is now generally accepted that the instrumental records do not cover the full range of hydroclimatic variability and any risk assessments based on them are likely to underestimate, or at least misinterpret, the frequency, duration, magnitude and timing of wet and dry periods (Ho et al., 2015; Tozer et al., 2016).

Proxy records provide indirect estimates of past local or regional hydroclimate, derived from natural archives such as sediment cores, speleothems, ice cores and tree rings (Croke et al., 2021). Access to palaeoclimate proxy databases offers the scientific community an opportunity to extend instrumental records back in time and better elucidate natural climate variability. Improving our understanding of such variability requires making use of statistical methods to understand relationships between palaeoclimate proxies and direct measurements of the hydroclimate over an instrumental time period. Armed with an understanding of the relationship over the instrumental period, we can extrapolate back through time to estimate and quantify uncertainty in a reconstruction period. Reconstructions of climate beyond the period of direct measurements have been performed in numerous studies that combine appropriate statistical methods and information from proxy records (Cahill et al., 2016; Hernández et al., 2020; Michel et al., 2020; Parnell et al., 2015).

Our paper provides details on a new approach to reconstructing the hydroclimate of selected catchments in Queensland, one of Australia's most climatically extreme states, using a set of hydroclimate indices and a newly-available palaeoclimate proxy database that has been compiled for the Australasian region (Croke et al., 2021). Croke et al. (2021) identified which of the 396 proxy records included in the database best correlate with a range of hydroclimate variables for Queensland catchments. Here, the application of this database is expanded by presenting a Bayesian time-series, multi-proxy, inverse modeling approach to produce reconstructions of hydroclimate indices at the catchment scale in Queensland.

The proposed framework establishes (1) the time-series characteristics of the hydroclimate, based on direct measurements between 1889 and 2017 (referred to as the instrumental period) and (2) the relationship between palaeoclimate proxies and the hydroclimate within the instrumental period. We use a state-space model with a first order autoregressive (AR) process to capture the variation in the hydroclimate over time and a quadratic regression to model proxy variation as a function of the hydroclimate. The past (unobserved) hydroclimate is subsequently reconstructed based on combining time series back-projection with inverse regression modeling (e.g., Cahill et al., 2016). The advantages of the approach are, firstly, it provides a standard method that can be applied at any and all locations for which the relevant data are available. Secondly, multiple proxies are used to inform the hydroclimate reconstruction, which means that strength is drawn from multiple data sources. Thirdly, the choice of what proxies to include is aided by a filtering approach which aims to remove proxy records that have poor modern analogues and finally, using a Bayesian framework holds a major advantage over other traditional methods (e.g., principal component regression, partial least squares and elastic net) used in this context (e.g., Cook et al., 2002; Luterbacher et al., 2001; Michel et al., 2020), as it is conceptually simpler to deal with missing data and to build a complex model which quantifies the relationship and uncertainties between multiple proxies and a climate variable.

2 | DATA AND STUDY AREA

The proxy and hydroclimate data used in this study was obtained from the PalaeoWISE (Palaeoclimate Data for Water Industry and Security Planning) database which comprises 396 quality-assured proxy records, their metadata, and their

relation to Queensland catchment hydroclimate (Croke et al., 2021). Proxy records in the database are derived from 11 different archive types (e.g., corals, tree rings, sediments, speleothems) providing both high- (≤1 year) and low- (>1 year) resolution. Further details on the number and range of proxy archives are presented in Croke et al. (2021).

The selected hydroclimate indices include average annual temperature, average annual rainfall, average annual evapotranspiration, Standardized Precipitation Index (SPI) (Adams, 2017; McKee et al., 1993), Standardized Precipitation-Evapotranspiration Index (SPEI) (Adams, 2017) and SPI- and SPEI-derived indices for extreme droughts and floods (McKee, Doesken, and Kleist 1993). Gridded datasets (cell size = 0.05 degrees, approximately 10 km) of instrumental rainfall, temperature and evapotranspiration were extracted from the Scientific Information for Landowners (SILO) database (https://www.longpaddock.qld.gov.au/silo) for the period 1889 to 2019 using the July to June water year. SPI and SPEI grids (cell size = 0.05 degrees) were then calculated from instrumental data at timescales of 12, 24, 36, and 48 months, which are standard accumulation periods used by hydrologists and climatologists. The relationship between the proxy records and catchment-averaged hydroclimate indices was tested in Croke et al., 2021 using correlation analysis across the whole PalaeoWISE database which found that proxies can have the highest correlations with hydroclimate time series at lags of anywhere between −5 and +5 years. The most appropriate time lag to use is also included in the database and this information is utilized in this study. Preliminary time series analysis for the instrumental hydroclimate indices was carried out using the fable and fpp3 R packages (O'Hara-Wild et al., 2021, Hyndman, Athanasopoulos & O'Hara-Wild, 2021) and the code for running the analysis is available in this vignette.

For the purposes of validating our statistical model we use the hydroclimate and proxy data associated with 18 catchment areas, including 8 in the Wet Tropics of Queensland, 9 in South East Queensland and 1 in Fitzroy (Figure 1).

However, when illustrating modeling results we focus specifically on two case-study catchments that demonstrate the variability in Queensland's hydroclimate: the sub-tropical, semi-arid Fitzroy catchment and the sub-tropical Brisbane
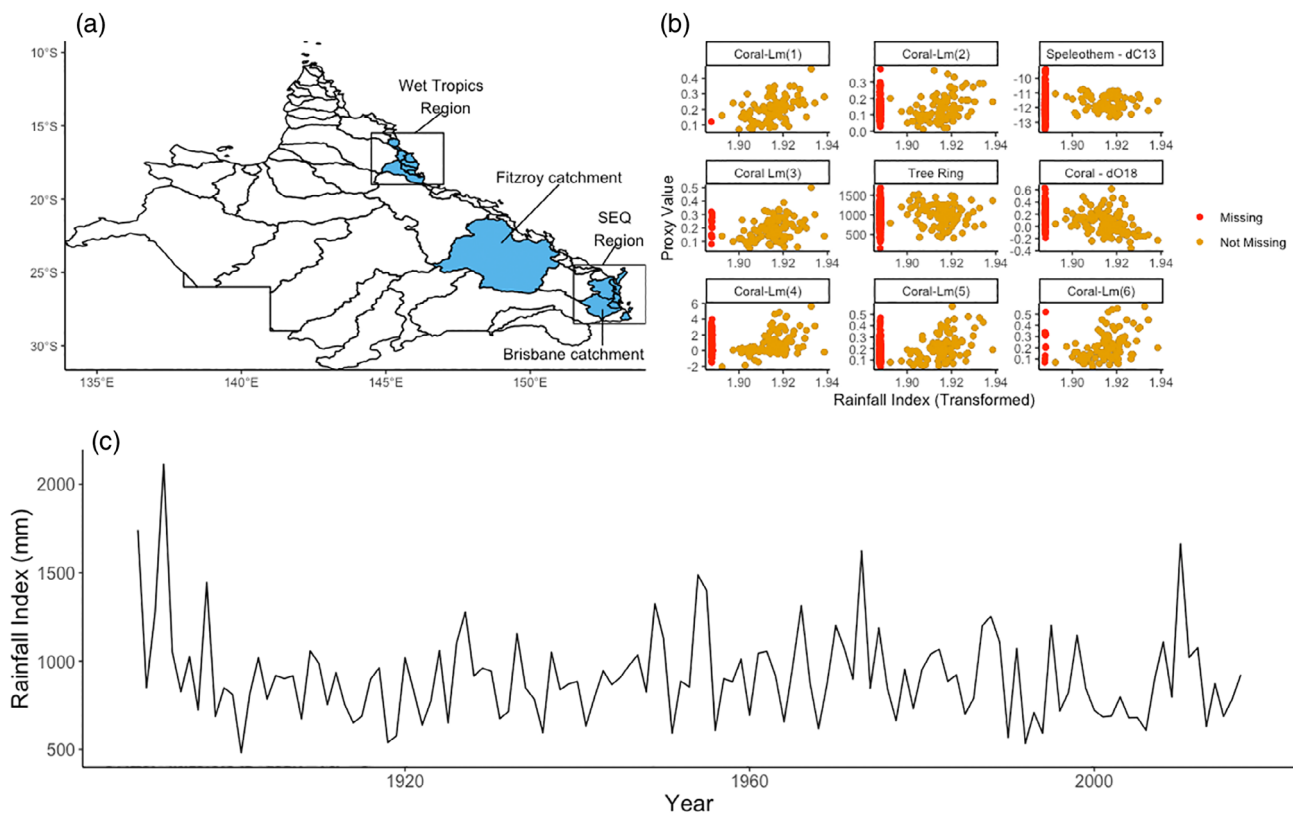
FIGURE 1 Map of Queensland and case study catchments and proxy records related to the rainfall index in the Brisbane catchment. (a) The 18 catchment areas used for the validation are shown in blue. Boxes highlight the Wet Tropics and the South East Queensland (SEQ) regions. Case study catchments Brisbane and Fitzroy are labeled. (b) Proxy records derived from corals, Tree rings, and Speleothems that have been shown to relate to the rainfall index in Brisbane. The orange points indicate the pairs of proxy and climate data that are available over the instrumental time period. The red points indicate the proxy data that are available over the reconstruction time period (i.e., when instrumental data is missing). (c) The rainfall index (RFI) plotted over the instrumental time period for the Brisbane catchment

catchment (Figure 1). The Fitzroy (~157,000 km ^{2}) catchment is the largest river catchment in Queensland, draining into the Great Barrier Reef lagoon, and is the largest cattle-producing region in Australia. The Brisbane catchment (13,500 km ^{2}) is the largest within the densely populated South East Queensland (SEQ) region (~ 27,000 km ^{2}), and supports extensive food production. Each catchment has a number of proxies associated with the various hydroclimate variables as determined by Croke et al. (2021). For example, Figure 1b shows the relationship between a number of proxies and average annual rainfall herein, the rainfall index (RFI), available for the Brisbane catchment. Figure 1c shows how the RFI has changed over the instrumental time period.

3 | METHODS

We propose a Bayesian model which relies on (1) a state-space model with mean modelled by a first order autoregressive (AR) process to capture the variation in a hydroclimate index over time and (2) a quadratic regression model to capture proxy variation across multiple different proxies as a function of the hydroclimate. Quantification of hydroclimate time-series dynamics and multiple proxy hydroclimate relationships using calibration data, combined with inverse modeling using historical proxy records, allows us to reconstruct the past hydroclimate drawing on information from multiple proxy input sources. We use simulation-based methods to infer all unknown quantities, including the past (unobserved) hydroclimate, parameters within the model, and uncertainties. The model is structured in a framework where data is represented at the data level, the unobserved (latent) quantities are represented at the process level and the parameters and hyper-parameters are represented at the parameter level. The method, described in detail below, can be implemented using the R code and data found in this Github repository.

We will begin by outlining our notation:

1. I_t is a hydroclimate measurement at time t. For the instrumental period (1889 to 2019) I_t is observed. For the reconstruction period, these are parameters to be estimated.
2. y_{ij} is j at time $t_{[i,j]}$, where $t_{[i,j]}$ is the time point corresponding to observation i of proxy j.
3. We superscript I and Y with c when referring to the instrumental time period, such that I^c and Y^c correspond to the hydroclimate measurements and proxy values that are available in the time period 1889 to 2019. We will refer to these data as the calibration data.
4. We subscript I and Y with r when referring to the reconstruction time period such that Y^r is the proxy data available in the reconstruction period and I^r is the reconstruction of the hydroclimate, to be estimated by the model.
5. γ_t is the latent state of the hydroclimate at time t.
6. ϕ is a set of parameters governing the dynamics of how γ changes over time, where $\phi = (\omega, \delta, \rho, \nu, \tau)$. These parameters, which will be defined in the methods section, are informed by the calibration data.
7. θ is a set of parameters governing the relationship between Y and the hydroclimate I, where for the jth proxy, $\theta_j = \alpha_j, \beta_{j,1}, \beta_{j,2}, \sigma_j$. These parameters, which will be defined in the methods section, are informed by the calibration data.

Note that all hydroclimate and proxy data were standardized to have mean 0 and variance 1 prior to inclusion in the model.

The rainfall index exhibits non-Gaussian behavior and is transformed using a Box-Cox transformation prior to analysis. The parameter of the Box-Cox transformation was chosen via maximum likelihood using the boxcox function from the MASS package (Ripley et al., 2021) in R. The transformation parameter estimate will vary depending on what catchment the rainfall index comes from. For the Brisbane catchment (Figure 1c), the transformation parameter estimate is −0.3.

3.1 | Data model

We will assume a univariate state-space model for the observed hydroclimate time series, where we model the hydroclimate with variability around some level γ, such that

$$I_t \sim N(\gamma_t, \tau^2),$$

The average hydroclimate γ_t will be modelled as time series process that will be defined in the process modeling section. The variability of I_t around γ_t is captured by τ^2.

The observed proxy data will be linked to their expected values, μ_{ij}, defined in the process modeling section, by assuming that

$$y_{ij} \sim N(\mu_{ij}, \sigma_j^2),$$

where σ_j^2 captures the variation of the observations around the modelled expectation for proxy j.

3.2 | Process model

We model the average hydroclimate time series process, γ_t, in one of two ways depending on the dynamics of the series. If there is an apparent trend in the time series then we model γ_t, with a systematic component, which is assumed to be linear, plus a time series component, η_t, which captures deviations away from the linear trend, such that,

$$\gamma_t = \omega + \delta t + \eta_t,$$

where the linear trend has intercept ω and slope δ. If there is no apparent trend in the series then

$$\gamma_t = \eta_t.$$

The time series, η_t, is modelled as a first order autoregression AR(1) process, such that

$$\eta_t \sim N(\rho\eta_{t-1}, v^2).$$

ρ is the autocorrelation parameter that determines how close consecutive values of η are to each other. We assume a stationary process such that $|\rho| < 1$, that is, dependence on the current state of the series becomes weaker as the distance over time increases. v^2 captures the random variation between η_t and $\rho\eta_{t-1}$.

We let μ_{ij}, the expected value of the ith observation of proxy j, be a quadratic function of the hydroclimate index at $t[i, j]$, where $t[i, j]$ is the time index associated with the ith observation of proxy j for $j = 1, \ldots, M$ proxies and $i = 1, \ldots, N_j$ time points for proxy j, where

$$\mu_{ij} = \alpha_j + \beta_{j,1} I_{t[i,j]} + \beta_{j,2} I_{t[i,j]}^2.$$

The $t[i, j]$ indexes are determined based on what lagged version of the hydroclimate time series is most correlated with proxy j. For example, if the ith observation of proxy j is observed at time point $t = 2$, and if proxy j is best correlated with the series with a lag of -1, then $t[i, j] = 1$. The data on what lags are used, as determined by Croke et al. (2021) can be found in this Github repository. Note the aim here is to ultimately reconstruct observations of I^r, not the latent state γ^r, and therefore μ_{ij} is set up as a function of I in order to achieve this via inverse prediction, which is covered in the next section.

3.3 | Inverse prediction via forward modeling

Noting that the proxy data, Y, decomposes into $Y = [Y^r, Y^c]$ and the time series, I, decomposes into $I = [I^r, I^c]$, and letting $\gamma = [\gamma^r, \gamma^c]$ be the vector containing the corresponding gamma elements where the superscripts r and c denote the reconstruction and calibration periods, respectively, the overall goal of the approach is to produce the joint posterior distribution

$$p(I^r, \gamma, \theta, \phi | I^c, Y^c, Y^r) \propto p(Y^c | I^c, \theta) p(Y^r | I^r, \theta) p(I^c | \gamma^c, \phi) p(I^r | \gamma^r, \phi) p(\gamma^c | \phi, \gamma^r) p(\gamma^r | \phi) p(\theta) p(\phi).$$

The term on the left-hand side of the equation is the posterior distribution and represents the probability distribution of the hydroclimate reconstruction given the observed instrumental data. The terms on the right-hand side represent respectively, the likelihood (the probability distribution of Y^c given I^c), the distributions of Y^r given I^r, I^c given γ^c and I^r given γ^r, and the prior distributions of the γ^c and γ^r processes and model parameters, θ and ϕ.

For the likelihood,

$$p(y_j^c|\theta, I^c) = \prod_{i=1}^{n_j^c} f_j(y_{ij}^c|I_{t[i,j]}^c, \theta_j),$$

where n_j^c is the number of observations for proxy j within the instrumental time period (1889 to 2019). The set of process and data model parameters are informed by the calibration data I^c and Y^c contained within this likelihood. In inverse prediction, the unknown I^r are added to the set of parameters that need to be estimated. y_j^r are observed and included in the likelihood, where

$$p(y_j^r|\theta, I^r) = \prod_{i=1}^{n_j^r} f_j(y_{ij}^r|I_{t[i,j]}^r, \theta_j)),$$

and

$$I_t^r|\gamma_t^r, \phi \sim N(\gamma_t^r, \tau^2),$$

where $\theta_j = (\alpha_j, \beta_{j,1}, \beta_{j,2}, \sigma_j)$ and $\phi = (\omega, \delta, \rho, \nu, \tau)$.

3.4 | Prior distributions

The parameters in the model are estimated in a Bayesian framework. Vague prior distributions are specified for α_j such that $\alpha_j \sim N(0, 2^2)$. This specification is considered to be vague - because the proxy data is standardized to have mean = 0 and variance = 1. Laplace priors are placed on the β_{k_j} coefficients such that $\beta_{k_j} \sim Laplace(0, \lambda)$. This is equivalent to a lasso regression, where a Laplace prior places a stronger confidence on zero than a normal prior centered on zero (e.g., Tibshirani, 1996). This prior specification helps to select coefficients for inclusion in the model, for example if the quadratic term is not strongly supported by the data it will essentially drop out of the model. We perform selection of the regularization parameter λ by putting a hyperprior on it, in this case a half-t prior centered on 0 with scale set at 10^2 and 1 degree of freedom. The hydroclimate linear trend parameter, δ, is given a non-informative normal prior centered on 0 with a variance 10^2. The autocorrelation parameter of the AR(1) time series process, ρ, is given a uniform prior between -1 and 1. The standard deviation of the AR(1) process and the data model standard deviation parameters (ν and σ_j) are given half-t priors centered on 0 with variance 2^2 and 1 degree of freedom. This specification is considered to be vague because the proxy data and the hydroclimate data is standardized to have variance = 1.

3.5 | Proxy filtering

Prior to running the model outlined above, a proxy filtering procedure is implemented. Palaeoclimate reconstructions are based on a modern analogue assumption so that modern relationships, derived from the overlap of proxy and observed climate data of the instrumental period, can be used to infer past climate states (e.g., Herbert and Harrison, 2016). Reconstructions rely on there being some degree of similarity between the range of proxy values associated with the instrumental and reconstruction periods (i.e., they need past analogues for the current proxy values) because calibration datasets suffer from severely restricted predictive power in "no modern analogue" situations (Horton & Edwards, 2005). Let $\overline{y}_j^c$ and s_j^c be the mean and standard deviation of the proxy calibration data (i.e., the data available over the instrumental time period) for proxy j, and let $\min(y_j^r)$ and $\max(y_j^r)$ be the minimum and maximum values of the reconstruction data (i.e., the data available over the reconstruction time period) for proxy j. We calculate a filtering measure based on how many standard deviations (s_j^c) the $\min(y_j^r)$ and $\max(y_j^r)$ are away from $\overline{y}_j^c$ such that

$$F_j = \max\left(\frac{|\overline{y}_j^c - \min(y_j^r)|}{s_j^c}, \frac{|\max(y_j^r) - \overline{y}_j^c|}{s_j^c}\right).$$
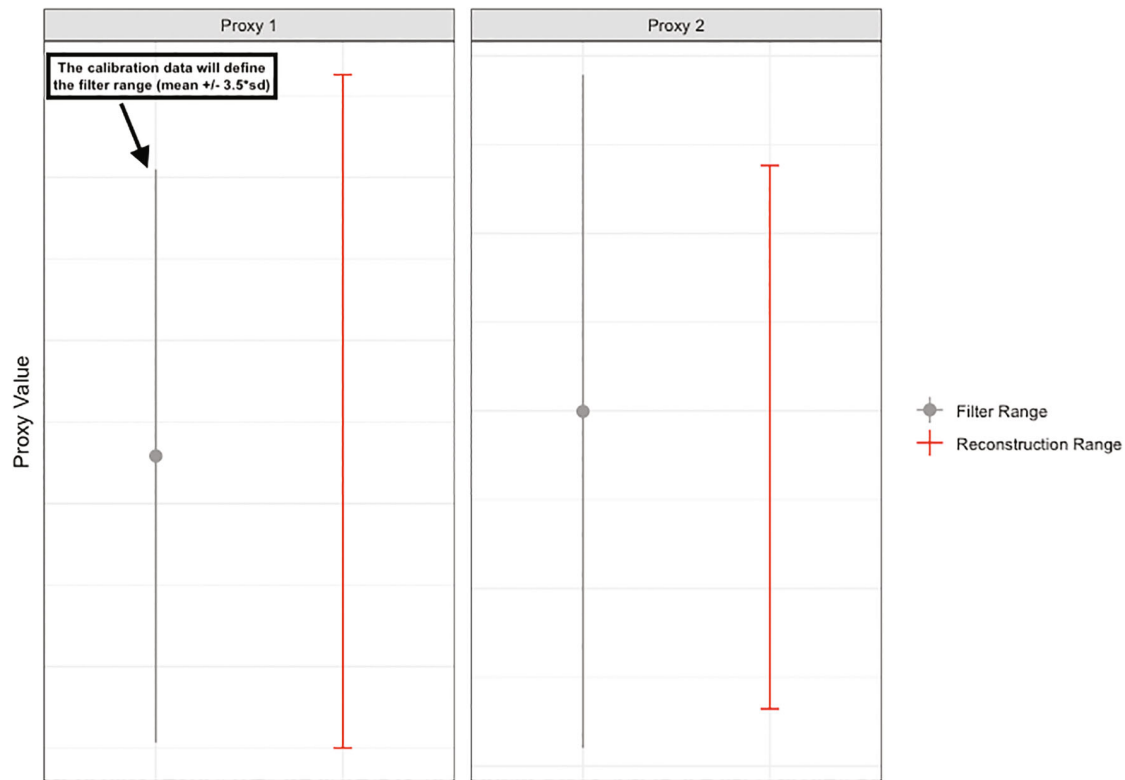
FIGURE 2 Illustration of the filtering criteria. The filtering range is shown with the grey vertical bars and is determined by the proxy calibration data. The grey point is the mean of the proxy calibration data. The range of the proxy reconstruction data is illustrated with the red horizontal bar. For Proxy 1, the maximum of the reconstruction data is more than 3.5 standard deviations away from the calibration data mean. Proxy 2 would not be filtered

If F_j is greater than 3.5 for proxy j, that is, if the minimum or the maximum proxy value in the reconstruction period is more than 3.5 standard deviations away from the instrumental period mean then we filter out the proxy record and it will not be used in the reconstruction. See Figure 2 for an illustration of the filtering procedure. Proxies are also filtered if they only contain one observation for the instrumental period. An example of the consequence of this filtering for reconstructing the RFI in the Brisbane catchment is that the Coral - Luminescence (1), Coral- δ O18 and the Speleothem - δ 13C proxies (Figure 1b), were excluded from the reconstruction model.

3.6 | Posterior inference

A Markov chain Monte Carlo (MCMC) algorithm is used to derive samples of the posterior distributions of the parameters of the model, including the reconstruction parameter I^r. The MCMC sampling algorithm is implemented using JAGS (Just Another Gibbs Sampler; Plummer, 2003). To evaluate the JAGS output we used 'rjags', an R package that offers cross-platform support from JAGS to the R interface (Plummer, Alexey, and Denwood, 2021). The results include a set of posterior trajectories for the hydroclimate reconstruction. The median of these results was taken to be the point estimate and a 95% credible interval was calculated using the 2.5% and 97.5% percentiles from the posterior distribution for the reconstructions in each year. The results are based on a run of 15,000 iterations, of which the first 5,000 are discarded and the remainder is thinned by saving every tenth sample. The algorithm is initialized from 3 different starting points yielding three chains containing 1000 samples (3000 samples in total) from the posterior distributions of the model parameters. Decisions on thinning were made to ensure an adequate effective sample size (ESS), such that the ESS would be at least 10% of the total number of samples. Convergence was checked using the R-hat diagnostics (e.g., Vehtari et al., 2021) and trace plots. R-hat values <1.1 were assumed to be an indicator of convergence.

3.7 | Estimating the probability of exceeding observed minimum/maximum values

We make use of the posterior samples of I_t^r to estimate the probability that the hydroclimate index in year t was lower (higher) than the minimum (maximum) hydroclimate value observed over the instrumental time period. Let $I_t^{r(s)}$ be a posterior sample of a reconstruction at time t and let p_t^- be the probability that a hydroclimate index value at time t in the reconstruction period was lower than the observed minimum (denoted I_{min}^c), such that

$$p_t^- = (1/N) \sum_{s=1}^{N} \mathbb{1}(I_t^{r(s)} < I_{min}^c),$$

where $\mathbb{1}$ is an indicator function such that $\mathbb{1}(x) = 1$ if the condition x holds true and 0 otherwise and N is the number of posterior samples used in the calculation. Similarly, let p_t^+ be the probability that a hydroclimate index at time t in the reconstruction period was higher than the observed maximum (denoted I_{max}^c), such that

$$p_t^+ = (1/N) \sum_{s=1}^{N} \mathbb{1}(I_t^{r(s)} > I_{max}^c).$$

4 | MODEL VALIDATION

We assess model performance via a validation exercise which focused on reconstructing 8 different hydroclimate indices for 18 catchment areas but leaving out some of the oldest observations from each index. Specifically, we leave out the 15 oldest data points from each hydroclimate index to use as test data for an out-of-sample validation. After leaving out these data we apply the proxy filtering (described in Section 3.5) and then fit the model to the training data set to obtain reconstruction estimates and 95% credible intervals for the test data set. We calculate coverage of the 95% credible intervals, mean errors and the root mean-squared error (RMSE) for the test data broken down by hydroclimate index (Table 1).

Note, not all catchment areas will be represented in the test data associated with each hydroclimate index and hence the sample sizes in Table 1 vary. In addition, the results are only presented for records that passed convergence checks. The mean error provides a measure of the average bias in the model predictions. Overall, the coverage of the 95% uncertainty intervals is 90%, suggesting that the reconstruction will capture the truth 90% of the time. The overall mean error, while close to zero is negative (−0.06) seen in Table 1 which indicates that on average the model is slightly biased towards

TABLE 1 Validation results

Climate variable	Description[a]	Coverage (target 95%)	Mean error	RMSE	N
All		90	**−0.06**	1.04	930
rain_1yr_wy7	Average annual rainfall	93	−0.16	1.05	180
avg_temp_1yr_wy7	Average annual temperature	91	0.11	0.99	150
spi_12m_1yr_wy7	SPI extreme flood index (12)	91	−0.13	1.09	150
spei_12m_1yr_wy7	SPEI extreme drought index (12)	90	0.01	1.09	150
spei_36m_1yr_wy7	SPEI extreme drought index (36)	90	−0.09	0.92	30
et_morton_potential_1yr_wy7	Evapotranspiration (Morton method)	89	−0.33	1.08	90
spei_24m_1yr_wy7	SPEI extreme drought index (24)	87	0.12	1.04	120
spei_48m_1yr_wy7	SPEI extreme drought index (48)	87	−0.05	0.84	60

Note: Summaries of cross-validation results based on standardized data are shown for hydroclimate indices in the test data set. Labels in the climate variable column are consistent with the PalaeoWise database. The results are only presented for records that passed convergence checks and are ordered based on coverage (highest to lowest). Coverage is defined as the percentage of time that the true value is captured with the 95% uncertainty intervals. The mean error is the average prediction error.

Abbreviations: N, number of datapoints; RMSE, root mean squared error; SPEI, standardized precipitation-evapotranspiration index; SPI, standardized precipitation index.

[a]Number in brackets indicates the aggregation period in months.

over-predicting the hydroclimate indices. The RMSE provides a summary of the variation in the prediction errors and can be interpreted as a standard deviation. Table 1 also indicates the variations in the validation measure when broken down by hydroclimate index. Coverage ranges from 87% to 93%. Ideally all coverage values would be 95%. The mean errors range from −0.33 to 0.12 with 5 of the indices showing a slight bias towards over prediction and the remainder showing a slight bias towards under prediction. The RMSE, which provides a measure of the spread of the prediction errors, ranges from 0.83 to 1.09.

5 | CASE STUDIES

This section focuses on applying the model to reconstruct two different climate indices (1) the rainfall index (RFI) and (2) the Standardized Precipitation Evapotranspiration Index with a 12 months aggregation period (SPEI (12)). We focus on reconstructing these indices for the Brisbane and Fitzroy catchment areas. The process model without the trend component was used. Table 2 provides a summary of the proxy data available for the reconstructions and the number of proxies that were filtered and illustrates that not all proxy records span the same time period. For example, some of the proxy records used in the reconstructions will have less of an overlap with the hydroclimate variables in the instrumental time period relative to others and each of the proxy records can be of different lengths and temporal resolutions. The length of a reconstruction will be determined by the length of continuous proxy coverage (in years) once filtering has been applied. The filtering procedure resulted in 3 proxies being excluded from informing the RFI in Brisbane (Coral-Luminescence (1),

TABLE 2 Data Summary

Catchment	Hydroclimate index	# Proxy records (before filter)	# Proxy records (after filter)	Range of proxy start-years (after filter)	Range of proxy end-years (after filter)	Instrumental period start-end	PalaeoWISE dataset ID (after filter)
Brisbane	RFI	9	6[a–c]	1876–1612	1984–2001	1889–2001	11[a], 2[a], 224[b], 269[c], 8[a], 9[a]
Fitzroy	RFI	22	18[a,c,d,e]	1881–1030	1983–2008	1889–2008	10[a], 11[a], 13[a], 14[a], 15[a], 16[a], 17[a], 2[a], 205[d], 245[e], 246[e], 269[a], 3[a], 4[a], 5[a], 6[a], 8[a], 9[a]
Brisbane	SPEI (12)	13	9[a–c]	1876–1612	1981–2001	1889–2001	11[a], 13[a], 15[a], 2[a], 224[b], 269[c], 4[25], 8[a], 9[a]
Fitzroy	SPEI (12)	21	18[a,c,e,f]	1881–1030	1981–2008	1889–2008	10[a], 11[a], 13[a], 14[a], 15[a], 16[a], 168[f], 17[a], 2[a], 245[e], 246[e], 269[c], 3[a], 4[a], 5[a], 6[a], 8[a], 9[a]

Note: A summary of the available proxy data related to the Rainfall Index (RFI) and the Standardized Precipitation-Evapotranspiration Index for a 12-months aggregation period (SPEI (12)) for the Brisbane and Fitzroy catchments. Columns 3 and 4 shows the number of proxy datasets before and after the filtering was applied. Columns 5 and 6 show the range of years where the proxy records begin and end. Column 7 shows the start and end points of the instrumental time period. Column 8 references the dataset IDs as they appear in the PalaeoWISE Database.

[a]Lough, J.M. Northeast Queensland 350 Year Summer Rainfall Reconstructions, NOAA National Centers for Environmental Information, 2011. https://www.ncdc.noaa.gov/paleo/study/10292.

[b]Palmer, J.G. Palmer - Waihora Terrace - PHTR - ITRDB NEWZ058, NOAA National Centers for Environmental Information, 2002. https://www.ncdc.noaa.gov/paleo-search/study/4083.

[c]Hendy, E.J., Gagan, M.K., Lough, J.M. Kurrimine Beach, Brook Island, Britomart Reef, Great Palm Island, Lodestone Reef, Pandora Reef, Havannah Island - Luminescence master chronology, NOAA National Centers for Environmental Information, 2003. https://www.ncdc.noaa.gov/paleo-search/study/1918.

[d]Xiong, L., Palmer, J.G. Xiong - Werberforce - LIBI - ITRDB NEWZ075, NOAA National Centers for Environmental Information, 2002. https://www.ncdc.noaa.gov/paleo-search/study/5378.

[e]Buckley, B.M., Anchukaitis, K.J., Cook, B.I., Canh Nam, Le. Buckley - Bidoup Nui Ba National Park - FOHO - ITRDB VIET001 NOAA National Centers for Environmental Information, 2010. https://www.ncdc.noaa.gov/paleo-search/study/10453.

[f]Urban, F.E., Cole, J.E., Overpeck, J.T. Maiana - Data, NOAA National Centers for Environmental Information, 2000. https://www.ncdc.noaa.gov/paleo-search/study/1859.

Coral-delta O18, Speleothem-delta C13; Figure 1). For the RFI reconstruction in Fitzroy, 4 proxies were excluded including 2 coral-luminescence proxies, a tree ring proxy and a coral-delta-Oxygen-18 proxy. For the SPEI (12) reconstructions, speleothem-delta-Carbon-13, coral-delta-Oxygen-18, tree ring and coral-luminescence proxies were excluded for Brisbane. Coral-luminescence, coral-delta-Oxygen-18 and a tree ring proxy were excluded for Fitzroy. This filtering limited the proxies here to just two archives, tree rings and coral luminescence, both of which have well-established physical mechanisms which describe their relationships to hydroclimate (Ho et al., 2015; Braganza et al. 2009). The RFI and SPEI (12) reconstructions extend back to 1612 CE and 1030 CE for the Brisbane and Fitzroy catchments respectively (Table 2).

In the next section we present probabilistic reconstructions and analysis of extremes values relative to observed minimum and maximum values over the instrumental period for the RFI and the SPEI (12) in case study catchments Brisbane and Fitzroy. Detailed annual model-based estimates (plus uncertainty) of the RFI and SPEI for these catchment areas are available here. Probabilistic reconstructions and detailed annual estimates (plus uncertainty) for other hydroclimate variables and catchment areas can be produced using our R code.
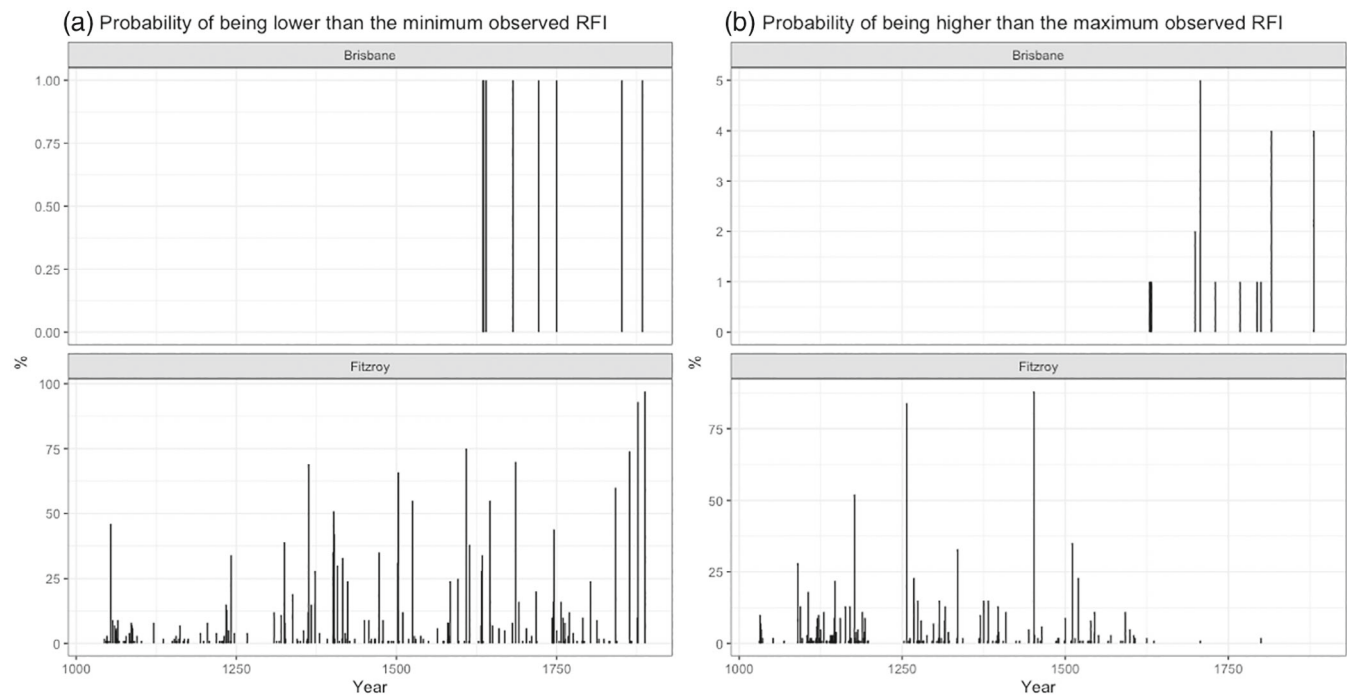
5.1 | Rainfall index reconstruction

Figure 3 shows RFI reconstructions (mm) for the Brisbane and Fitzroy catchments. In the Brisbane catchment, on average the estimated RFI over the reconstruction period is lower than the average observed RFI over the instrumental period (a value of 892 mm compared to 926 mm). The reconstruction period estimates also exhibit less variability than the observed RFI, with a standard deviation of 158 mm for the reconstruction period compared to 259 mm for the instrumental period. In the Fitzroy catchment, the average estimated RFI for the reconstruction period is 667 mm compared to 678 mm for the instrumental period. The reconstruction period estimates exhibit slightly less variability than the observed RFI, with a standard deviation of 195 mm compared to 198 mm. It is worth noting that the start of the instrumental period in these catchments coincided with the timing of some of the largest floods on record (Bureau of Meteorology, 2017).

In Figure 4 we make use of the probabilistic nature of the reconstructions by using the uncertainty to identify how likely RFI was to exceed observed minimum/maximum values (i.e., observed during the instrumental period) in any given year during the reconstruction period.
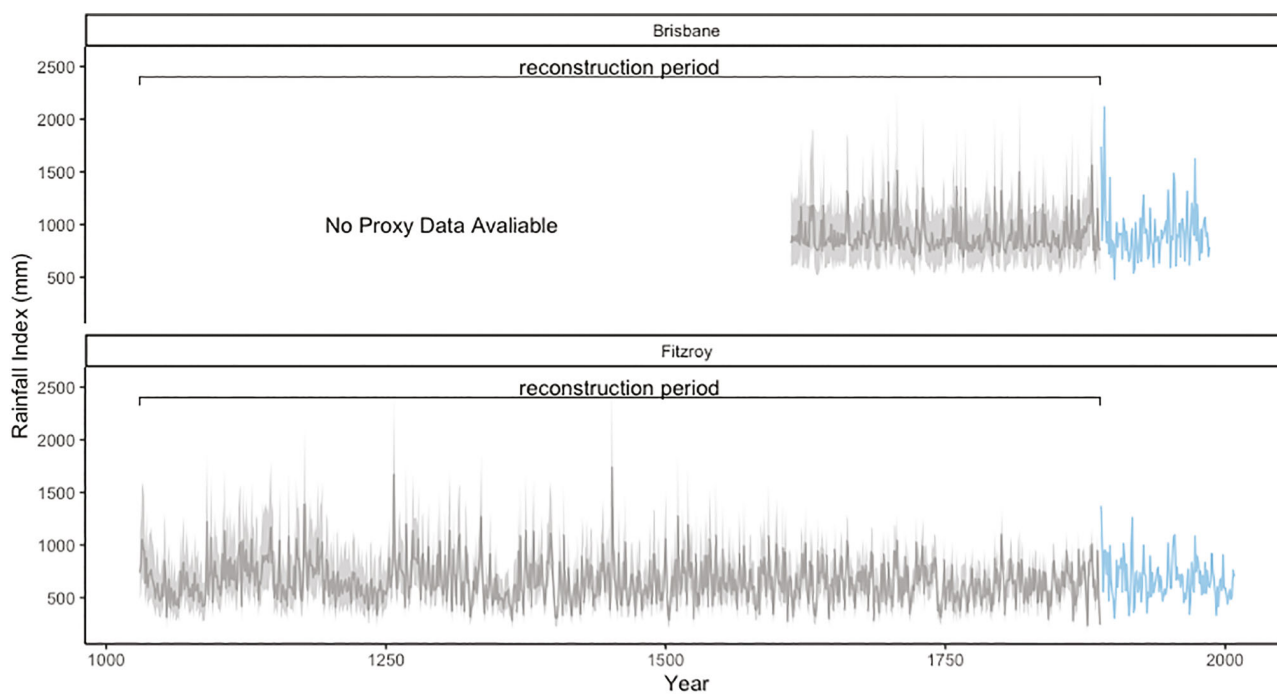
FIGURE 3 Rainfall Index (RFI) in mm reconstructions for the Brisbane and Fitzroy catchment areas. The solid blue line represents the observed instrumental data. The solid grey lines are the model-based estimates with the shaded grey areas representing 95% uncertainty intervals for the reconstruction period

FIGURE 4 The probability of Rainfall Index (RFI) extremes for the Brisbane and Fitzroy catchment areas. The bars in (a) indicate the probability of RFI in a given reconstruction year being lower than the minimum RFI observed in the instrumental period. The bars in (b) indicate the probability of RFI in a given reconstruction year being higher than the maximum RFI observed in the instrumental period

Figure 4a shows the probability of the RFI in the reconstruction time period being less than the observed minimum between 1889 and 2019 for Brisbane and Fitzroy catchments. Conversely, Figure 4b shows the probability of the RFI in the reconstruction time period being greater than the observed maximum.

According to the model based reconstruction for Brisbane (reconstruction period: 1612–1888), the RFI is unlikely to have fallen below the minimum observed RFI in any year (all probabilities are below 1%). The reconstruction also shows the RFI was unlikely to have exceeded the observed maximum (all probabilities were less than 5%). In the Fitzroy catchment (reconstruction period: 1030–1888), the chance of RFI falling below the minimum observed RFI exceeds 50% in 11 years of the reconstruction period and exceeds 75% in 2 of those years (1877 and 1888). The RFI is likely to have exceeded the maximum observed RFI in 3 years during the reconstruction period (1177, 1257 and 1452; >50% probability).
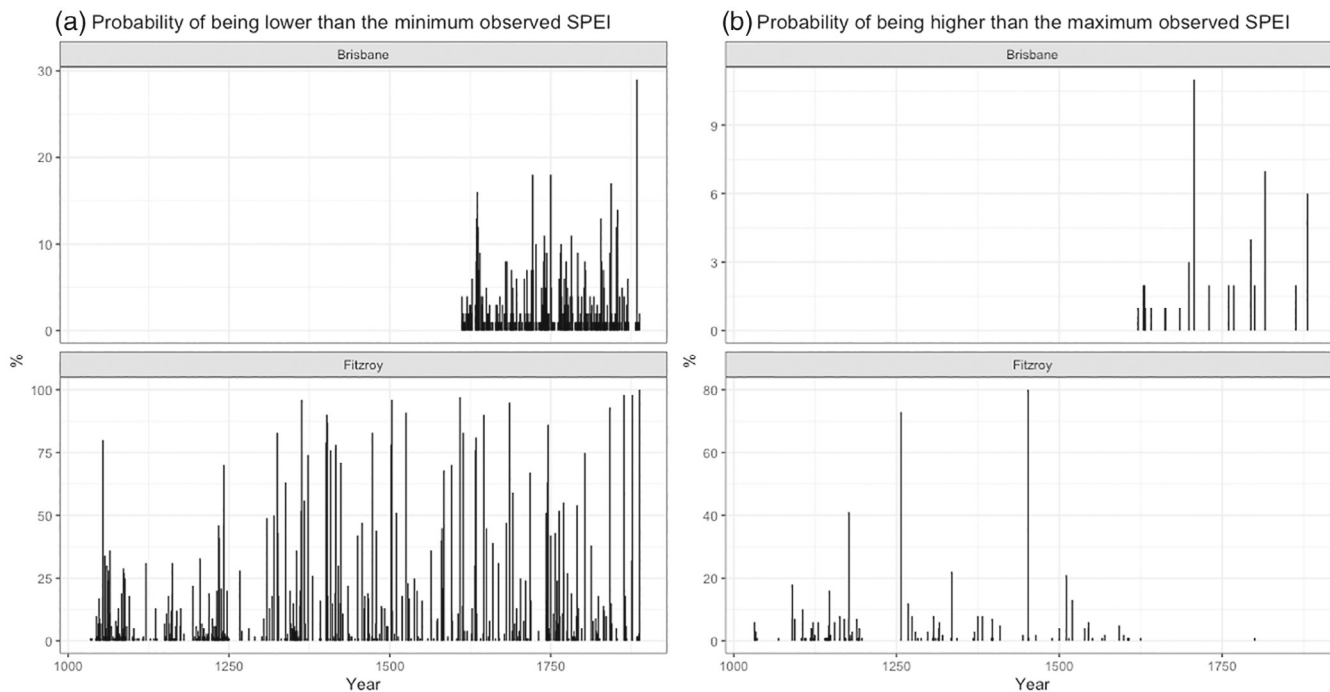
5.2 | Standardized precipitation-evapotranspiration index reconstruction

Figure 5 shows SPEI (12) reconstructions for the Brisbane and Fitzroy catchments. In Brisbane, the average estimated SPEI for the reconstruction period is the same as the average over the instrumental period (a value of 0.1). However, as with the RFI, the reconstruction period estimates exhibit less variability with a standard deviation of 0.7 for the reconstruction period compared to 1.1 for the instrumental. In Fitzroy, the average estimated SPEI is 0 over both the reconstruction and instrumental periods. The reconstruction period estimates of SPEI exhibit similar variability to the observed SPEI, with a standard deviation of 1.04 compared to 1.06.

In terms of analyzing exceedance of observed minimums/maximums, Figure 6a,b show the probability of SPEI (12) in the reconstruction time period being lower (higher) than the observed minimum (maximum) between 1889 and 2017 for the Brisbane and Fitzroy catchments. According to the reconstruction for Brisbane (reconstruction period: 1612–1888), the chance that the SPEI fell below the minimum or above the maximum observed SPI is below 30% for all years. In Fitzroy (reconstruction period: 1030–1888) the chance of SPEI falling below the minimum observed SPEI exceeds 50% in 40 years of the reconstruction period. The chance of SPEI falling above the maximum observed SPEI is greater than 50% in only 2 years of the reconstruction period (1257 and 1452).
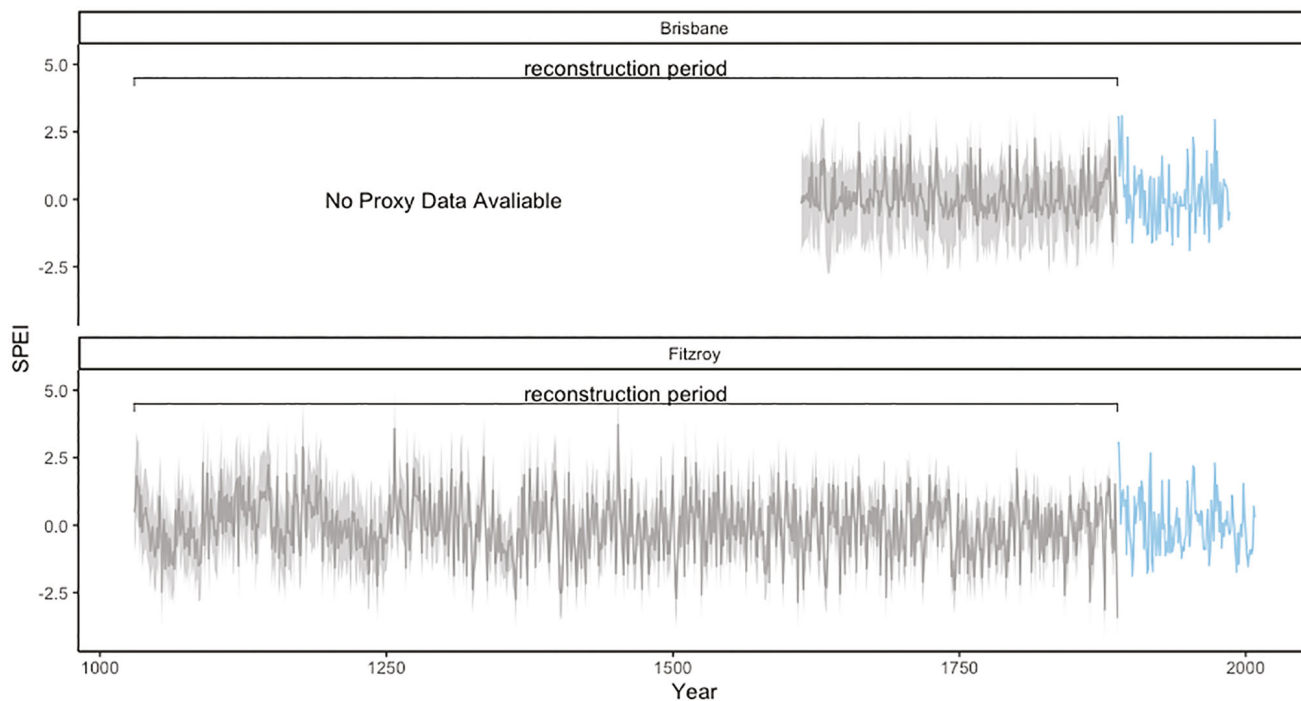
FIGURE 5 Standardized Precipitation-Evapotranspiration Index (SPEI) reconstructions for the Brisbane and Fitzroy catchment areas. The solid blue line represents the observed data. The solid grey lines are the model-based estimates for the reconstruction period and the shaded grey areas represent 95% uncertainty intervals for the reconstruction

FIGURE 6 The probability of Standardized Precipitation-Evapotranspiration Index (SPEI) extremes for the Brisbane and Fitzroy catchment areas. The bars in (a) indicate the probability of SPEI in a given reconstruction year being lower than the minimum SPEI observed in the instrumental period. The bars in (b) indicate the probability of SPEI in a given reconstruction year being higher than the maximum SPEI observed in the instrumental period

6 | DISCUSSION

Improving the management of drought, flood, water security and hydroclimatic risk requires an understanding of long-term climate variability. Reconstructions of rainfall, temperature and climate drivers, such as ENSO, from proxy data are not new and in recent years there has been much attention on how such data can contribute to flood and drought risk planning. There is a general acceptance by the water security industry that palaeoclimate proxy data has an important role to play in future predictions of climate which is reflected in the general uptake by industry and local governments. This reflects the general consensus that the post-1900 instrumental period (i.e., the period on which all water resources infrastructure, policy, operation rules and strategies is based) does not capture the full range of variability that has occurred. For example, in the state of New South Wales (NSW), regional water strategies include specific use of palaeoclimate data in the stochastic modeling to quantify climate variability and inform on climatic extremes such as floods and droughts (NSW Department of Planning, Industry and Environment, 2020). In particular, it uses the high-resolution record from the Law Dome ice cores in Antarctica, which have been used to identify eight mega-droughts (lasting from 5 to 39 years) during 1000–2009 AD (Vance et al., 2015).

Until recently, palaeoclimate proxy data were often stored in inaccessible journal papers. The construction of the PalaeoWISE database was the first step in providing easy access to quality-assured, standardized proxy data of relevance to Australia (Croke et al., 2021). It also provides details on how selected proxy data correlate with the hydroclimate indices of Queensland, allowing a user to see which proxy data may be best to focus on in any subsequent analysis.

To date there is no standardized approach to using multiple palaeoclimate proxy records for hydroclimate reconstructions. Previous work has tended to use single proxy records and different statistical techniques of varying complexity. Each method, regardless of proxy type, will rely on a set of assumptions regarding the relationships between proxy variables and the climate indices to be reconstructed (e.g., Birks et al. 2012). For example, the utilization of transfer functions for deriving palaeohydrological reconstructions from testate amoebae assemblages is now commonplace in several regions of the world (Amesbury et al., 2016; Krashevska et al., 2020; Schnitchen et al., 2006; Swindles et al., 2015). Recently, diatom-based transfer function have been used for producing quantitative palaeoclimatic reconstructions in Southwest China (Zou et al., 2021). Principal component regression has been used in streamflow reconstructions from tree-ring chronologies (E. R. Cook et al., 1999; Hidalgo et al., 2001). Faraji et al. (2021) employed principal component analysis to obtain reliable annual hydrological variability from speleothems. Vance et al. (2013) used spectral analysis, which allows for the study of the periodic behavior of time series, to explore changes in El Niño-Southern Oscillation and rainfall variability in eastern Australia based on a 1010-yr record of Law Dome summer sea salts (Vance 2012). Our approach adds further value to the widespread adoption of palaeoclimate proxy data as a vital data source on long term water planning in Australia. We note below several advantages of our proposed approach.

6.1 | Using a standardized statistical methodology with multiple proxies

Our approach avails of the largest database of palaeoclimate proxy data for the southern hemisphere. The database includes a total of 396 proxies that have been shown to correlate with a selected range of hydroclimate indices across numerous geographic locations in Australia. While we limit this paper to two case study locations, our method can be viewed as a standard approach that can be applied at any and all locations for which the relevant data are available. The statistical model takes a relatively straightforward approach to quantifying the relationship between proxies and hydroclimate indices using standard regression and time series techniques for data calibration within the instrumental period and reconstruction beyond the instrumental period. The model allows for the inclusion of multiple proxies for informing the hydroclimate reconstruction, which means that we can draw strength from multiple data sources in an attempt to quantify the uncertainty around past changes. The choice of what proxies to include is aided by our filtering approach which helps us to remove proxy records that have poor modern analogues. However, there is flexibility within the model that still allows for the inclusion/exclusion of proxies to be user defined. This flexibility comes with the caveat that model convergence checks must be carried out on the results.

6.2 | The advantage of a Bayesian approach

Our model fits within a Bayesian framework which relies on the use of MCMC algorithms to generate samples of the unknown parameters in our statistical model. After convergence, these samples provide the posterior distributions for

any parameter in the model or any quantity which is a function of these parameters, including, in our case, distributions for hydroclimate reconstructions. Once we have access to these posterior distributions we can very easily obtain point estimates, quantiles and summaries, for example posterior medians and 95% credible intervals. A major advantage of the Bayesian MCMC approach is its flexibility. It is relatively straightforward to fit models to complex data sets with measurement error, missing observations, multilevel or serial correlation structures, and multiple endpoints. It is usually much more difficult to develop the frequentist (non-Bayesian) procedures for fitting such models. In our case, the Bayesian framework also provides a convenient setting for inverse modeling, that is, where we wish to predict the value of the independent hydroclimate variable from observations of the dependent proxy variable. We achieve this in our model by establishing the dependence between the variables over an instrumental time period and then placing a prior on the "missing" independent variables over the reconstructions period. Another notable advantage of the Bayesian analysis approach is that the uncertainty is handled by default within the model due to the parameters being defined from prior probability distributions. Once the data model is combined with the prior distributions to obtain the posteriors for the parameters, we automatically have information on the reliability of the estimates. The uncertainty in those estimates is propagated through any function of the parameters which in our case includes the hydroclimate reconstruction.

6.3 | Limitations of the approach

Our proposed modeling approach is not without limitations, which can be summarized in three main points.

1. This method suffers from the same issue that all reconstruction approaches do, which is that it relies on the assumption that the proxy-climate relationship remains constant in time. This is a ubiquitous problem with proxies, as the proxy variability will not solely be controlled by the climate indicator of interest. However, this problem is mitigated somewhat in our method since multiple proxy sources are used in the hydroclimate reconstruction and thus the resulting hydroclimate estimates will be informed by multiple proxy-hydroclimate relationships, not just a single proxy-hydroclimate relationship.

2. The proxy filtering approach uses a threshold value of 3.5 which is user defined. This value was chosen to strike a balance between removing too many proxies and keeping proxies that cause modern analogue issues which can result in model convergence problems. We would like to note that results may be sensitive to the choice of threshold. If users wish to be more conservative in terms of proxy removal, the filtering value can be increased, and this might decrease the number of proxies that are excluded from the model. Note, that the change may lead to model convergence problems, in which case the 3.5 threshold is recommended.

3. The method does not provide an automatic convergence diagnosis. Convergence diagnostic measures must be checked by the user on a case by case basis. MCMC settings for the number of iterations may need to be adjusted in cases where convergence is not achieved, which will increase the computation time.

4. The quadratic component of the model could be viewed as simplistic and non-parametric regression approaches might allow for more flexibility. However, the potential increase in prediction accuracy that might be obtained with the increase in flexibility is not enough to warrant the substantial computational burden that would make the use of this model more difficult in a practical sense.

5. This model does not explore spatial dependencies in the hydroclimate indices and it does not allow for assumptions that individual proxy variation might be controlled by multiple hydroclimate indices at the same time. These would be realistic modeling assumptions to make, and we see future work as extending this method to account for these more complex assumptions. However, this model was specifically developed for efficiency and as a first step to giving users the ability to reconstruct independent climate indices using multiple proxy sources.

6.4 | Potential applications to the water security industry

The direct cost of restricted water availability to Australian urban and rural business is estimated to be as high as $A15 billion per year during droughts (or ∼1.6% of Australia's GDP; Dept. Agriculture and Environment (2021)). Water restrictions in major cities during the millennium drought cost ∼$A815 million per year and affected more than 80% of Australian households (Dept. Agriculture and Environment, 2021. Following amendments to the Queensland Water Act in 2018, water related climate change effects on water availability, water use practices and the risk to land or water resources

arising from use of water on land must be considered in the preparation of water plans. The Act also requires best practice science to be used. Therefore, there is an increasing need to understand the full range of natural climatic variability, particularly on decadal and longer timescales (Head et al., 2014) and questions inevitably arise as to whether resource assessments that are based on the recorded recent past are robust. In the absence of direct measurements, reconstructions such as those presented in our case study section can ultimately be used to reassess current or baseline flood/drought risks and quantify what should be considered "normal" and "extreme" based on longer-term past variability.

It has been common, for example, in water resource assessments to calculate the "historical no-failure yield" which essentially tests the system's performance against the worst drought in recorded history. However, important questions arise as to whether there were likely to have been drought events prior to the recorded data period that are worse and can we quantify the uncertainty around such events. As we have demonstrated, reconstructions derived from our methodology could be used to answer such questions and ultimately improve water resource assessments through highlighting exposures to extreme events worse than have been recorded and through the appropriate quantification of uncertainties related to estimating such exposures. For example, according to our model based reconstructions, in Brisbane the RFI is unlikely (probabilities between 0% and 5%) to have exhibited extremes beyond the minimum/maximum of what has been observed between 1889 and 2019. However, in Fitzroy there are a number of years during the reconstruction period where the RFI is likely (>50% probability) to have exhibited behavior beyond the minimum/maximum of what has been observed. For SPEI, the probability of observing extremes beyond the minimum/maximum of what has been observed since 1889 doesn't exceed 50% in any reconstruction year in the Brisbane catchment -but exceeds 50% in multiple years for the Fitzroy catchment.

The next step is to make these reconstructions available to the water industry to incorporate into water resource modeling. Identifying solutions for hydroclimatic risk adaptation strategies that are both optimal and robust in the presence of uncertainty presents a difficult challenge. Reconstructions are a critical foundational data from which a range of derivates can be extracted. Of specific relevance to water resource modeling applications, the annual based reconstructions can be disaggregated into daily data for model input. Additionally, the time series can readily be classified according to different criteria to identify events of interest for example, which were the 10 driest years, decades, or centuries. This highlights the versatility of catchment scale climate reconstructions to help answer a wide range of questions that will help improve our understanding of the longer-term context within which known historical (i.e., instrumental) climate exists as well as a point of comparison with future projections of climate. For example, SEQ has previously experienced water scarcity, when the main storage reservoir at Wivenhoe Dam fell below 15% during the Australian Millennium Drought. The longer palaeoclimate reconstructions produced here can now be used assess how often a Millennium Drought might occur using existing rainfall-runoff derived model outputs. This is an approach also proposed by other states such as New South Wales (NSW) where the Department of Planning, Industry and Environment is reviewing the usability of this palaeoclimate data for town water security assessments under the Safe and Secure Water program (NSW Department of Planning, Industry and Environment, 2020).

It is important to stress that all reconstructions must be used in a manner suitable for the end-user. For water resource management, the reconstruction's time series form the input data to existing hydrological models. In other instances, the reconstructions can be used to re-calculate risk or to determine notable changes in climate patterns over this longer centennial timescale. The methodology outlined in this paper is the first to avail of all proxy data in the PalaeoWISE database to help reconstruct climate indices of relevance to the water industry and to help make these freely available for operational scenarios of relevance to critical business decisions.

DATA AVAILABILITY STATEMENT

ORCID

Niamh Cahill https://orcid.org/0000-0003-3086-550X
Micheline Campbell https://orcid.org/0000-0002-9626-1189

REFERENCES

Adams, J. (2017). Climate indices, an open source python library providing reference implementations of commonly used climate indices. https://github.com/monocongo/climate_indices

Amesbury, M. J., Swindles, G. T., Bobrov, A., Charman, D. J., Holden, J., Lamentowicz, M., Mallon, G., Mazei, Y., Mitchell, E. A. D., Payne, R. J., Roland, T. P., Turner, T. E., & Warner, B. G. (2016). Development of a new pan-European testate amoeba transfer function for reconstructing peatland palaeohydrology. *Quaternary Science Reviews*, *152*, 132–151. https://doi.org/10.1016/j.quascirev.2016.09.024

Armstrong, M. S., Kiem, A. S., & Vance, T. R. (2020). Comparing instrumental, paleoclimate, and projected rainfall data: Implications for water resources management and hydrological modeling. *Journal of Hydrology: Regional Studies*, *31*, 100728. https://doi.org/10.1016/j.ejrh.2020.100728

Birks, H. J. B., Heiri, O., Heikki, S., & Bjune, A. E. (2012). Strengths and weaknesses of quantitative climate reconstructions based on late-quaternary biological proxies. *The Open Ecology Journal*, *3*, 68–110. https://doi.org/10.2174/1874213001003020068

Braganza, K., Gergis, J. L., Power, S. B., Risbey, J. S., & Fowler, A. M. (2009). A multiproxy index of the El Niño–Southern Oscillation, A.D. *Journal of Geophysical Research: Atmospheres*, *114*(D5), 1525–1982. https://doi.org/10.1029/2008JD010896

Bureau of Meteorology. (2017). *Known floods in the brisbane & bremer river basin*. Australian Government http://www.bom.gov.au/qld/flood/fld_history/brisbane_history.shtml

Cahill, N., Kemp, A. C., Horton, B. P., & Parnell, A. C. (2016). A Bayesian hierarchical model for reconstructing relative sea level: From raw data to rates of change. *Climate of the Past*, *12*(2), 525-542. https://doi.org/10.5194/cp-12-525-2016

Cook, B. I., Palmer, J. G., Cook, E. R., Turney, C. S. M., Allen, K., Fenwick, P., O'Donnell, A., Lough, J. M., Grierson, P. F., Ho, M., & Baker, P. J. (2016). The paleoclimate context and future trajectory of extreme summer hydroclimate in eastern Australia. *Journal of Geophysical Research: Atmospheres*, *121*(21), 12812–20838. https://doi.org/10.1002/2016JD024892

Cook, E. R., D'Arrigo, R. D., & Mann, M. E. (2002). A well-verified, multiproxy reconstruction of the winter north atlantic oscillation index since A.D. 1400. *Journal of Climate*, *15*(13), 1754–1764. https://doi.org/10.1175/1520-0442(2002)015%3C1754:AWVMRO%3E2.0.CO;2

Cook, E. R., Meko, D. M., Stahle, D. W., & Cleaveland, M. K. (1999). Drought reconstructions for the continental United States. *Journal of Climate*, *12*(4), 1145–1162. https://doi.org/10.1175/1520-0442(1999)012%3C1145:DRFTCU%3E2.0.CO;2

Croke, J., Vítkovský, J., Hughes, K., Campbell, M., Amirnezhad-Mozhdehi, S., Parnell, A., Cahill, N., & Dalla Pozza, R. (2021). A paleoclimate proxy database for water security planning in Queensland Australia. *Scientific Data*, *8*(1), 292. https://doi.org/10.1038/s41597-021-01074-8

Dept. Agriculture, Water, and the Environment. (2021). *Drought policy*. Australian Governement https://www.awe.gov.au/agriculture-land/farm-food-drought/drought/drought-policy

Dixon, B. C., Tyler, J. T., Henley, B. J., & Drysdale, R. (2019). *Regional patterns of hydroclimate variability in southeastern Australia over the past 1200 years. Earth and Space Science Open Archive.* https://doi.org/10.1002/essoar.10501482.1

Dowdy, A. J., Pepler, A., Di Luca, A., Cavicchia, L., Mills, G., Evans, J. P., Louis, S., McInnes, K. L., & Walsh, K. (2019). Review of Australian east coast low pressure systems and associated extremes. *Climate Dynamics*, *53*(7), 4887–4910. https://doi.org/10.1007/s00382-019-04836-8

Faraji, M., Borsato, A., Frisia, S., Hellstrom, J. C., Lorrey, A., Hartland, A., Greig, A., & Mattey, D. P. (2021). Accurate dating of stalagmites from low seasonal contrast tropical Pacific climate using Sr 2D maps, fabrics and annual hydrological cycles. *Scientific Reports*, *11*(1), 2178. https://doi.org/10.1038/s41598-021-81941-x

Head, L., Adams, M., McGregor, H. V., & Toole, S. (2014). Climate change and Australia. *WIREs Climate Change*, *5*(2), 175–197. https://doi.org/10.1002/wcc.255

Herbert, A. V., & Harrison, S. P. (2016). Evaluation of a modern-analogue methodology for reconstructing Australian paleoclimate from pollen. *Review of Paleobotany and Palynology*, *226*, 65–77. https://doi.org/10.1016/j.revpalbo.2015.12.006

Hernández, A., Sánchez-López, G., Pla-Rabes, S., Comas-Bru, L., Parnell, P., Cahill, N., Geyer, A., Trigo, R. M., & Giralt, S. (2020). A 2000-year Bayesian NAO reconstruction from the Iberian Peninsula. *Scientific Reports*, *10*(1), 14961. https://doi.org/10.1038/s41598-020-71372-5

Hidalgo, H. G., Piechota, T. C., & Dracup, J. A. (2001). Alternative principal components regression procedures for dendrohydrologic reconstructions. *Surface Water and Climate*, *36*(11), 3241-3249.

Ho, M., Kiem, A. S., & Verdon-Kidd, D. C. (2015). A paleoclimate rainfall reconstruction in the Murray-Darling Basin (MDB), Australia: 1. Evaluation of different paleoclimate archives, rainfall networks, and reconstruction techniques. *Water Resource Research*, *51*(10), 8380-8396.

Horton, B. P., & Edwards, R. J. (2005). The application of local and regional transfer functions to reconstruct former sea levels, North Norfolk, England. *The Holocene*, *15*, 216–228.

Hyndman, R, Athanasopoulos, G, and O'Hara-Wild, M. 2021. "*fpp3: forecasting: principles and practice*". R package version 0.4.0.

Kiem, A. S., Vance, T. R., Tozer, C. R., Roberts, J. L., Dalla Pozza, R., Vitkovsky, J., Smolders, K., & Curran, M. A. J. (2020). Learning from the past – Using paleoclimate data to better understand and manage drought in South East Queensland (SEQ), Australia. *Journal of Hydrology: Regional Studies*, *29*, 100686. https://doi.org/10.1016/j.ejrh.2020.100686

Krashevska, V., Tsyganov, A. N., Esaulov, A. S., Mazei, Y. A., Hapsari, K. A., Saad, A., Sabiham, S., Behling, H., & Biagioni, S. (2020). Testate amoeba species- and trait-based transfer functions for reconstruction of hydrological regime in tropical peatland of Central Sumatra, Indonesia. https://www.frontiersin.org/article/10.3389/fevo.2020.00225

Luterbacher, J., Xoplaki, E., Dietrich, D., Jones, P. D., Davies, T. D., Portis, D., Gonzalez-Rouco, J. F., von Storch, H., Gyalistras, D., Casty, C., & Wanner, H. (2001). Extending North Atlantic oscillation reconstructions back to 1500. *Atmospheric Science Letters*, *2*(1-4), 114–124. https://doi.org/10.1006/asle.2002.0047

McKee, T. B., Doesken, N. J., & Kleist, J. (1993). The relationship of drought frequency and duration to time scales. Paper presented at: Eighth Conference on Applied Climatology, American Meteorological Society.

Michel, S., Swingedouw, D., Chavent, M., Ortega, P., Mignot, J., & Khodri, M. (2020). Reconstructing climatic modes of variability from proxy records using ClimIndRec version 1.0. *Geoscientific Model Development*, *13*(2), 841–858. https://doi.org/10.5194/gmd-13-841-2020

NSW Department of Planning, Industry and Environment. 2020. "*Regional water strategies in New South Wales.*" NSW Department of Planning, Industry and Environment. https://www.industry.nsw.gov.au/water/plans-programs/regional-water-strategies.

O'Donnell, A. J., McCaw, W. L., Cook, E. R., & Grierson, P. F. (2021). Megadroughts and pluvials in southwest Australia: 1350–2017 CE. *Climate Dynamics*, *57*, 1817–1831. https://doi.org/10.1007/s00382-021-05782-0

O'Hara-Wild, M., Hyndman, R., Wang, E., Caceres, G., Hensel, T. G., & Hyndman, T. (2021). "fable: forecasting models for tidy time series.

Parnell, A. C., Sweeney, J., Doan, T. K., Salter-Townshend, M., Allen, J. R. M., Huntley, B., & Haslett, J. (2015). Bayesian inference for paleoclimate with time uncertainty and stochastic volatility. *Journal of the Royal Statistical Society: Series C (Applied Statistics)*, *64*(1), 115–138. https://doi.org/10.1111/rssc.12065

Plummer, M. (2003). JAGS: a program for analysis of Bayesian graphical models using Gibbs sampling. https://mcmc-jags.sourceforge.io

Plummer, M., Alexey, S., & Denwood, M. (2021). rjags: Bayesian graphical models using MCMC. R package version 4-12.

Ripley, B. D., Venables, W. N., Hornik, K., Gebhardt, A., & Firth, D. (2021). MASS: modern applied statistics with s. R package version 7.3-54. http://www.stats.ox.ac.uk/pub/MASS4/

Schnitchen, C., Charman, D. J., Magyari, E., Braun, M., Grigorszky, I., Tóthmérész, B., Molnár, M., & Szántó, Z. (2006). Reconstructing hydrological variability from testate amoebae analysis in Carpathian peatlands. *Journal of Paleolimnology*, *36*(1), 1–17. https://doi.org/10.1007/s10933-006-0001-y

Suncorp Group. 2013. "*Risky business: insurance and natural disaster risk management.*" Suncorp Group. https://www.google.com/url?sa=t&rct=j&q=&esrc=s&source=web&cd=&ved=2ahUKEwjg8bKshM3yAhUeRUEAHWmRCZoQFnoECAIQAQ&url=https%3A%2F%2Fwww.aph.gov.au%2Fparliamentary_business%2Fcommittees%2Fhouse_of_representatives_committees%3Furl%3Djscna%2Fsubs%2Fsub0151-%252.

Swindles, G. T., Holden, J., Raby, C. L., Turner, T. E., Blundell, A., Charman, D. J., Menberu, M. W., & Kløve, B. (2015). Testing peatland water-table depth transfer functions using high-resolution hydrological monitoring data. *Quaternary Science Reviews*, *120*, 107–117. https://doi.org/10.1016/j.quascirev.2015.04.019

Tibshirani, R. (1996). Regression shrinkage and selection via the lasso. *Journal of the Royal Statistical Society. Series B (Methodological)*, *58*(1), 267–288 http://www.jstor.org/stable/2346178

Tingstad, A. H., Groves, D. G., & Lempert, R. J. (2014). Paleoclimate scenarios to inform decision making in water resource management: example from southern California's inland empire. *Journal of Water Resources Planning and Management*, *140*(10), 4014025. https://doi.org/10.1061/(ASCE)WR.1943-5452.0000403

Tozer, C. R., Vance, T. R., Roberts, J. L., Kiem, A. S., Curran, M. A. J., & Moy, A. D. (2016). An ice core derived 1013-year catchment-scale annual rainfall reconstruction in subtropical eastern Australia. *Hydrology Earth System Sciences*, *20*(5), 1703–1717. https://doi.org/10.5194/hess-20-1703-2016

Vance, T. R. (2012). *Annualized summer sea salt from the law dome ice core chemistry record, 1000-2009, Ver. 1. Australian Antarctic Data Centre.* https://doi.org/10.26179/5d50ef2192dc4

Vance, T. R., Roberts, J. L., Plummer, C. T., Kiem, A. S., & van Ommen, T. D. (2015). Interdecadal pacific variability and eastern Australian megadroughts over the last millennium. *Geophysical Research Letters*, *42*(1), 129–137. https://doi.org/10.1002/2014GL062447

Vance, T. R., van Ommen, T. D., Curran, M. A. J., Plummer, C. T., & Moy, A. D. (2013). A millennial proxy record of ENSO and eastern Australian rainfall from the law dome ice core, East Antarctica. *Journal of Climate*, *26*(3), 710–725. https://doi.org/10.1175/JCLI-D-12-00003.1

Vehtari, A., Gelman, A., Simpson, D., Carpenter, B., & Bürkner, P. C. (2021). Rank-normalization, folding, and localization: an improved $\widehat{R}$ for assessing convergence of MCMC (with discussion). *Bayesian Analysis*, *16*(2), 667–718. https://doi.org/10.1214/20-BA1221

Zou, Y., Wang, L., He, H., Liu, G., Zhang, J., Yan, Y., Gu, Z., & Zheng, H. (2021). Application of a diatom transfer function to quantitative paleoclimatic reconstruction — a case study of Yunlong Lake, Southwest China. https://www.frontiersin.org/article/10.3389/feart.2021.700194